Rapid Fusion of Synaptic Vesicles with Reconstituted Target SNARE Membranes

Volker Kiessling,[†] Saheeb Ahmed,[‡] Marta K. Domanska,[†] Matthew G. Holt,[‡§] Reinhard Jahn,[‡] and Lukas K. Tamm[†*]

[†]Center for Membrane Biology and Department of Molecular Physiology and Biological Physics, University of Virginia, Charlottesville, Virginia; [‡]Department of Neurobiology, Max Planck Institute for Biophysical Chemistry, Göttingen, Germany; and [§]VIB Center for the Biology of Disease, K.U. Leuven Center for Human Genetics, Leuven, Belgium

ABSTRACT Neurotransmitter release at neuronal synapses occurs on a timescale of 1 ms or less. Reconstitution of vesicle fusion from purified synaptic proteins and lipids has played a major role in elucidating the synaptic exocytotic fusion machinery with ever increasing detail. However, one limitation of most reconstitution approaches has been the relatively slow rate of fusion that can be produced in these systems. In a related study, a notable exception is an approach measuring fusion of single reconstituted vesicles bearing the vesicle fusion protein synaptobrevin with supported planar membranes harboring the presynaptic plasma membrane proteins syntaxin and SNAP-25. Fusion times of ~20 ms were achieved in this system. Despite this advance, an important question with reconstituted systems is how well they mimic physiological systems they are supposed to reproduce. In this work, we demonstrate that purified synaptic vesicles from rat brain fuse with acceptor-SNARE containing planar bilayers equally fast as equivalent reconstituted vesicles and that their fusion efficiency is increased by divalent cations. Calcium boosts fusion through a combined general electrostatic and synaptotagmin-specific mechanism.

INTRODUCTION

Reconstitution of membrane fusion using purified components in model systems has played a major role in discovering the essential elements of the intracellular fusion apparatus and in elucidating how this complex machinery works (1–6). Most progress in this field has been made with the reconstitution of neuronal SNARE-mediated fusion, i.e., the process that is responsible for the exocytotic activity of synaptic vesicles to release neurotransmitters into the synaptic cleft between neurons. Although there is broad consensus in the field that the neuronal SNAREs synaptobrevin 2 (VAMP 2, Syb2) on the vesicle membrane and syntaxin 1a (Syx1a) and SNAP-25 on the presynaptic target membrane constitute the minimal fusion machinery in this system, many quite significant behaviors of physiological neuronal exocytosis are not well captured in the reconstituted systems. For example, neuronal exocytosis is highly regulated by calcium, but physiological calcium regulation is not well reproduced in the reconstituted systems that include the neuronal calcium regulator synaptotagmin 1 (Syt1) (7–10), although important progress has been made recently in this regard (11–13).

A second issue with the reconstitution of intracellular membrane fusion has been that ensemble assays of fusion typically produce fusion rates that are five orders of magnitude slower than synaptic exocytosis. This problem has been partially overcome by several groups that have developed a range of single-vesicle fusion assays (14–18). In these assays it is important to show that fusion depends on the known required neuronal SNARE composition. Domanska et al (17) were the first to reproduce SNARE-dependent fusion of single reconstituted vesicles to planar target membranes on a timescale of a few milliseconds, which approaches the speed of regulated synaptic fusion to within one order of magnitude. A major advantage is that docking and fusion can be distinguished and analyzed separately in this and related single-vesicle fusion assays. Furthermore, excellent control over diffusion of the reconstituted fusion proteins can be achieved in appropriately prepared planar target membranes. Therefore, these assays have become powerful tools in recent years to dissect the precise mechanistic roles of various regulatory proteins in calcium-controlled neuronal exocytosis.

Despite such progress, it needs to be born in mind that biological membranes are much more complex than artificial membranes containing only a few molecular species. Thus, the question remains to which extent observations made with such reconstituted systems are indeed faithfully reproducing the molecular events underlying docking and fusion in a synapse. In particular, docking in the reconstituted assays is mediated by the SNARE proteins that form *trans* complexes between the membranes, whereas in the synapse a host of other proteins are involved (19), with the role of SNAREs in docking being controversial. Fusion of docked vesicles may also be differently regulated in native membranes. For these reasons it is important to establish whether the fusion reactions measured with synthetic vesicles resemble those of native biological vesicles such as synaptic vesicles.

To address this issue, we have taken advantage of a recently established in vitro system in which SNARE-mediated

Submitted January 25, 2013, and accepted for publication March 22, 2013.

*Correspondence: lkt2e@virginia.edu

Editor: Huey Huang.

0006-3495/13/05/1950/9 $2.00

http://dx.doi.org/10.1016/j.bpj.2013.03.038

docking and fusion between vesicles and a planar supported membrane can be measured with high spatial and temporal resolution (17). To this end, we have now measured the docking and fusion of purified synaptic vesicles from rat brain and compared these measurements with similar experiments on reconstituted vesicles containing either Syb2 only or both Syb2 and Syt1 at physiological concentrations with acceptor SNAREs that were reconstituted in planar target membranes. We find that synaptic vesicles specifically dock to and readily fuse with reconstituted acceptor SNARE-containing planar membranes within milliseconds. Docking and fusion of synaptic vesicles is only partially dependent on calcium in this system, despite the presence of endogenous synaptotagmin in the membrane of synaptic vesicles, in agreement with the notion that additional factors are required in synapses to prevent fusion of docked vesicles in the absence of calcium.

MATERIALS AND METHODS

Materials

The following materials were purchased and used without further purification: bPC (L-α-phosphatidylcholine (porcine brain)), bPE (L-α-phosphatidylethanolamine (porcine brain)), bPS (L-α-phosphatidylserine (porcine brain)), bPIP$_2$ (L-α-phosphatidylinositol-4,5-bisphosphate (porcine brain)), Rh-DOPE (1,2-dioleoyl-*sn*-glycero-3-phosphoethanolamine-*N*-(lissamine rhodamine B sulfonyl) (Avanti Polar Lipids, Alabaster, AL); cholesterol, octyl-beta-D-glucopyranoside, EDTA, $CaCl_2$, and glycerol (Sigma Chemical, St. Louis, MO); CHAPS (Anatrace); HEPES, KCl (Research Products International); chloroform, ethanol, Contrad detergent, all inorganic acids, bases, and hydrogen peroxide (Fisher Scientific, Fair Lawn, NJ). Water was purified first with deionizing and organic-free 4 filters (Virginia Water Systems, Richmond, VA) and then with a NANOpure system from Barnstead (Dubuque, IA) to achieve a resistivity of 18.2 M/cm.

Protein expression and purification

SNARE proteins from *Rattus norvegicus* cloned in pET28a vector were expressed in BL21(DE3) *Escherichia coli* and purified as described previously (20,21). The cysteine-free variant of SNAP-25A consisted of residues 1–206 and Syb2 constructs included residues 49–96 or 1–117 with C-terminal cysteine (Cys-117). The acceptor SNARE complex (containing Syx1a, SNAP-25, and Syb49–96) was purified from BL21(DE3) expressing all three proteins, using the pET28a vector for SNAP-25A and the pETDuet-1 vector for Syx183–288 and Syb49–96. The complex and full-length Syb2 were purified by Ni^{2+}-NTA affinity chromatography followed by ion exchange chromatography using MonoQ or MonoS columns in the presence of 15 mM CHAPS (10).

Full-length Syt1 cloned in pET28a vector was expressed in BL21(DE3) CodonPlus-RIL *E. coli*. Protein was purified using standard Ni^{2+}-NTA affinity and ion exchange chromatography followed by size-exclusion chromatography using a Superdex200 column all in the presence of 0.03% *n*-dodecyl-β-D-maltoside. In the final step of purification after His-tag cleavage a second ion exchange was used in the presence of 15 mM CHAPS (10).

Synaptic vesicle purification

Synaptic vesicles from rat brain were purified as described previously (22). Briefly, rat brains were homogenized in homogenization buffer (320 mM sucrose, 4 mM HEPES-KOH, pH 7.4) in a glass-Teflon homogenizer. The homogenate was centrifuged at 1,000 $\times$ *g* for 10 min, the resulting supernatant was again centrifuged at 15,000 $\times$ *g* for 15 min. Synaptosomes were osmotically lysed with ice-cold water and homogenized with 3 strokes at 2000 rpm in a homogenizer. The lysate was centrifuged at 25,000 $\times$ *g* for 20 min to obtain LS1 fraction. LS1 was further centrifuged at 200,000 $\times$ *g* for 2 h. The resulting LP2 fraction was resuspended in 40 mM sucrose and layered on top of a continuous sucrose gradient (from 0.05 to 0.8M sucrose) and centrifuged at 65,000 $\times$ *g* for 4 h. Synaptic vesicles were collected at the interface of 0.8–1.2 M sucrose and further purified on a size-exclusion chromatography column (controlled pore glass beads).

Synaptic vesicle labeling

5–10 μl of a 1 mg/ml stock solution of Rh-DOPE in chloroform were evaporated under a stream of N_2 gas, while gently vortexing in a glass tube, followed by vacuum for at least 1 h. One aliquot of 50 μl synaptic vesicles (2.83 μg/μl) was thawed on ice and added to the dried, labeled lipid. After gentle vortexing for 5–10 min the sample was left in a 37°C water bath for ~30 min. Some samples were then washed 1–3 times in 600 μl reconstitution buffer (RB100, 20 mM HEPES, 100 mM KCl, pH 7.4 adjusted with KOH) by repeated centrifugation at 16,168 $\times$ *g* for 5 min at 4°C (5415R, Eppendorf, Hamburg, Germany) and resuspension steps. Omitting this step could be tolerated despite a higher background during single vesicle measurements. Finally, the sample volume was adjusted to 200 μl, kept on ice, and was used for five experiments on the same day.

Syb2 and Syt1 reconstitution into proteoliposomes

Syb2 and Syt1 were reconstituted into bPC/bPE/bPS/Chol/Rh-DOPE (26.5:27.5:5:40:1) proteoliposomes. Briefly, the desired lipids were mixed and organic solvents were evaporated under a stream of N_2 gas followed by vacuum for at least 1 h. The dried lipid films were dissolved with 1 mol % β-octylglucoside in reconstitution buffer (RB200, 20 mM HEPES, 200 mM KCl, pH 7.4 adjusted with KOH) followed by the addition of an appropriate volume of proteins to reach a final volume of ~180 μl and the desired protein/lipid ratios (Syb2 p/l 1:300, Syt1 p/l 1:1000). After 1 h of equilibration at room temperature, the mixture was diluted below the critical micellar concentration by adding more RB200 to a final volume of 550 μl. For content labeling, the fluorescent lipid analog DiD was used instead of Rh-DOPE and 70 mM sulforhodamine was added to the previous buffers. Detergent was removed on a G-50 superfine Sephadex (GE Healthcare) column and by dialyzing overnight against 500 ml of RB200 at 4°C with one change of buffer. This method results in unilamellar vesicles with diameters between 40 and 50 nm as determined by dynamic light scattering.

Acceptor SNARE complex reconstitution into proteoliposomes

Acceptor SNARE complex Syx1a(183–288)/SNAP25/Syb2(49–96) (ΔN complex) was reconstituted into bPC/bPE/bPS/bPIP$_2$/Chol (32:30:15:3:20) vesicles with a protein/lipid ratio of 1:3000 by rapid dilution of micellar protein/lipid/detergent mixtures followed by dialysis as described previously (17). For experiments with synaptic vesicles and Syb2/Syt1-proteoliposomes, the acceptor-SNARE proteoliposomes were prepared in RB100 and RB200, respectively.

SNARE reconstitution into planar supported bilayers

Planar supported bilayers with reconstituted SNAREs were prepared by a combined Langmuir-Blodgett/vesicle fusion technique as previously described (17,23,24). Briefly, quartz slides were cleaned by boiling in

Contrad detergent for 10 min, hot bath-sonicated while still in detergent for 30 min, followed by extensive rinsing with milliQ water. The slides were then immersed in three volumes of 95% H_2SO_4 to one volume of 30% H_2O_2, followed by extensive rinsing in milliQ water. Immediately before use, slides were further cleaned for 1–2 min in an argon plasma sterilizer (Harrick Scientific, Ossining, NY). The first leaflet of the bilayer was prepared by Langumir-Blodgett transfer. To do so, a lipid monolayer (bPC/Chol 4:1) was spread from a chloroform solution onto a pure water surface in a Nima 611 Langmuir-Blodgett trough (Nima, Conventry, UK). The solvent was allowed to evaporate for 10 min, before the monolayer was compressed at a rate of 10 cm^2/min to reach a surface pressure of 32 mN/m. After equilibration for 5–10 min, a clean quartz slide was rapidly (200 mm/min) dipped into the trough and slowly (5 mm/min) withdrawn, while a computer maintained a constant surface pressure and monitored the transfer of lipids headgroups down onto the hydrophilic substrate.

To complete the bilayer, a solution of proteoliposomes or protein-free vesicles (77 μM total lipid in 1.3 ml, which is a little more than the volume of the holding cell) was added and incubated at room temperature for 2 h. Excess unfused vesicles were then removed by perfusion with 10 ml RB followed by 5 ml RB containing either 1 mM $CaCl_2$, 1 mM EDTA, or 1 mM $MgCl_2$.

Total internal reflection fluorescence (TIRF) microscopy

Experiments were carried out on two fluorescence microscopes, a Zeiss Axiovert 35 and a Zeis Axiovert 200 (Carl Zeiss, Thornwood, NY), equipped with a 63× water immersion objective (Zeiss; N.A. = 0.95) and prism-based TIRF illumination with a characteristic penetration depth $d_p \approx 103$ nm. The light sources were two argon ion lasers (Innova 300C and Innova 90C, Coherent, Palo Alto, CA) emitting light at 514 nm. Fluorescence was observed through a 610-nm band-pass filter (D610/60, Chroma, Brattleboro, VT) by an electron multiplying CCD (DU-860E, Andor-Technologies, South Windsor, CT). The EMCCD was cooled to −70°C and the gain was typically set to an electron gain factor of ~200. For dual color experiments a diode laser (Cube 640, Coherent) was used as an additional light source and a dualview (Andor-Technologies) was used to separate the fluorescence from membrane and content dyes. The prism-quartz interface was lubricated with glycerol to allow easy translocation of the sample cell on the microscope stage. The beam was totally internally reflected at an angle of 72° from the surface normal. An elliptical area of 250 × 65 μm was illuminated. The intensity of the laser beam was computer-controlled through an acousto optic modulator (AOM-40, IntraAction, Bellwood, IL and Isomet, Springfield, VA) or could be blocked entirely by a computer-controlled shutter. The laser intensity, shutter, and camera were controlled by a homemade program written in LabVIEW (National Instruments, Austin, TX).

Single synaptic vesicle fusion assay

Supported acceptor SNARE bilayers were perfused with 1 ml of diluted membrane-labeled synaptic vesicle solution (40 μl synaptic vesicles in 1 ml RB100) on the microscope stage. Data acquisition was started ~1 min after the beginning of vesicle injection. Images of 127 × 127 $pixel^2$ (corresponding to a sample area of 46.7 × 46.7 μm^2) were acquired with an exposure time of 4 ms and a cycle time of 4.01 ms in series of 15,000 images in frame-transfer mode and spooled directly from the CCD camera to the hard drive. From one supported membrane preparation we collected 8–10 min of data.

Single proteoliposome fusion assay

Supported acceptor SNARE bilayers were perfused with 3 ml of 0.6 μM Syb2/Syt1 proteoliposomes containing 1 mol % labeled lipids (Rh-DOPE) mixed with 3.3 μM protein-free vesicles in RB200 on the microscope stage (concentration refers to total lipid). Image acquisition was performed as described above for synaptic vesicles. The fast imaging period was followed by ~30 min of single image acquisition to measure additional vesicle docking in bulk mode (17).

Analysis of single vesicle/liposome fusion and docking

Images were analyzed using a homemade program written in LabView (National Instruments). First, the whole stack of images was filtered by a moving average filter. The intensity maximum for each pixel over the whole stack was projected on a single image. Vesicles were located in this image by a single particle detection algorithm described previously (25). The peak (central pixel) and mean fluorescence intensities of a 5 × 5 $pixel^2$ area around each identified center of mass were plotted as a function of time for all particles in the 15,000 images of each series. The exact time points of docking and fusion were determined from the central pixel (17). For proteoliposomes experimentally obtained docking curves were fitted with first-order kinetics according to

$$D(t) = D_\infty\left(1 - e^{-k_{on}t}\right), \quad (1)$$

where D_∞ is the final concentration of occupied docking sites and k_{on} is the docking rate. Because of rhodamine residues in solution, this method could not be used to determine docking of synaptic vesicles. We therefore used the total numbers of observed docking events during the fast imaging period to quantify the amount of binding. Numbers were normalized to one standard condition (RB100 with 1 mM Ca^{2+}) to account for small differences in total vesicle concentration after labeling and washing. We define the fusion efficiency as the fraction of vesicles/liposomes that undergo fusion after docking. We report docking and fusion efficiency data as averages with standard deviations from at least five experiments under each condition.

Fusion kinetics analysis

Delay times between docking and onset of fusion were determined as previously described (17). Cumulative distributions of these lag times were analyzed using first-order kinetics with one (synaptic vesicles) or two (proteoliposomes) fractions according to

$$N(t) = N_1\left(1 - e^{-\frac{t}{\tau_1}}\right) + N_2\left(1 - e^{-\frac{t}{\tau_2}}\right), \quad (2)$$

where τ_1 and τ_2 are the characteristic time constants of fusion for two fractions and, N_1 and N_2 are the respective total numbers of events. Equation 2 was fitted to the data, starting at time 8 ms; this was necessary because in many cases it was not possible to accurately determine the delay times of events that happened within the first two imaging frames after docking. The graphs (see Fig. 3) were normalized with the fit results for N_1+N_2 and the fusion efficiencies.

RESULTS

Docking of synaptic vesicles and Syb-proteoliposomes depends on the presence of SNAREs

Previously, we observed fast SNARE-mediated vesicle fusion in an assay consisting of a plasma membrane-mimicking planar supported membrane and synaptic vesicle mimicking proteoliposomes (17,26). Here, we have adapted

this assay to compare docking and fusion reactions of Syb2 and Syt1 containing proteoliposomes with those of synaptic vesicles purified from rat brain. In both cases, the preformed acceptor SNARE complex Syx1a(183–288)/SNAP25/Syb2(49–96) (ΔN complex) (27) is reconstituted in an environment composed of lipids extracted from porcine brain consisting of close to physiological concentrations of PC, PE, PS, PIP_2, and cholesterol.

Proteoliposomes were labeled by adding Rh-DOPE to the lipid/protein/detergent mix from which the liposomes were formed by gel filtration. In contrast, synaptic vesicles were labeled by adding a small aliquot of Rh-DOPE to purified synaptic vesicles from rat brain, followed by extensive washing in buffer. This procedure was optimized to observe the fluorescence of single vesicles with good signal/noise for up to 10 min as they approached the surface of the supported planar membrane under TIRF illumination.

With acceptor SNARE complex present in the supported membrane, we observed docking and fusion events of single synaptic vesicles. Peak and mean intensities of 5 × 5 pixel regions around each immobilized vesicle were extracted. Fig. 1 depicts four examples of typical intensity traces. The time axis has been adjusted so that docking, which is characterized by a sharp increase of the mean and peak intensities, aligns with time point zero. We quantified docking by counting all recognized docking events and normalized the data with the result of the number of events in the presence of 1 mM Ca^{2+}, which was used as a standard. This normalization was necessary because the quantity of synaptic vesicles after labeling varied between different days. Fig. 2 *A* shows the mean relative docking of synaptic vesicles to acceptor SNARE membranes in the presence of 1 mM EDTA or 1 mM Ca^{2+}. The error bars represent the standard deviation of five to eight independent experiments. Although we did not observe a significant influence of calcium ions, docking is increased 5- to 10-fold when compared to control experiments with protein-free supported bilayers. Vesicle binding was also inhibited by the addition of Syb1–96 to the acceptor SNARE membrane.

Because of the different labeling procedure, the docking of proteoliposomes containing Syb2 and Syt1 can be observed over a longer time (17) and can be quantified more accurately. Fig. 2 *B* shows the relative docking to acceptor SNARE membranes in the presence of 1 mM Ca^{2+} or 1 mM EDTA as well as control experiments with Syb1-96 and protein-free membranes. As previously described for Syb2 only (i.e., without Syt1) proteoliposomes (17), docking is SNARE dependent. We did not detect any differences in docking between the different salt conditions. However, it is important to point out that because we are using very low vesicle concentrations, our assay is not optimized to quantify docking probabilities.

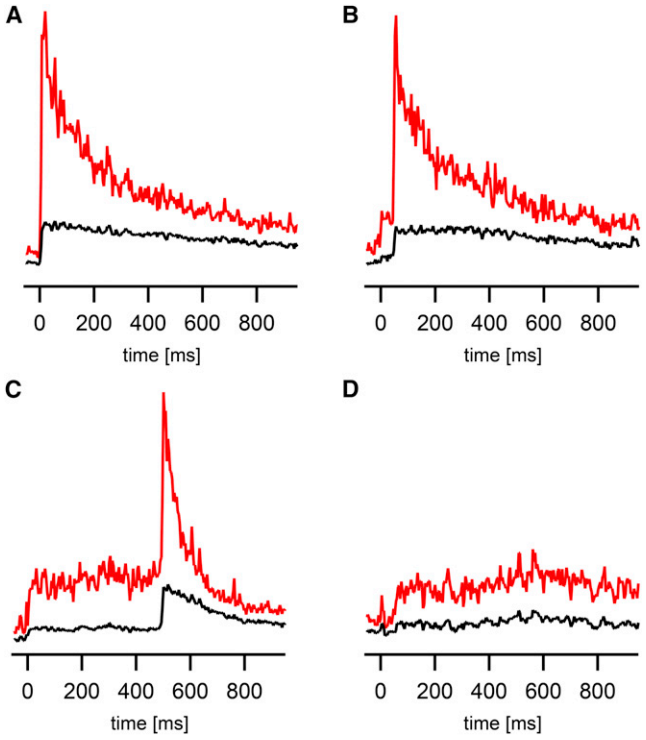

FIGURE 1 Examples of synaptic vesicle docking and fusion events to acceptor SNARE complex-containing supported membranes. Peak (*red*) and mean (*black*) fluorescence of 1.9 × 1.9 μm^2 regions around each vesicle were plotted. Time point zero was set to the time of docking characterized by a sharp increase of fluorescence. The onset of fusion is characterized by a second sharp increase of the intensity followed by an immediate decrease of the peak intensity and a delayed decrease of the mean intensity due to diffusion of Rh-DOPE out of the observed region. In (*A*) membrane fusion happens within the first frames after/during docking. In (*B*) the onset of fusion happens ~50 ms after docking. In (*C*) the onset of fusion happens ~500 ms after docking. In (*D*) only docking and no membrane fusion were observed.

Fast synaptic vesicle fusion with acceptor SNARE supported planar membranes

Membrane merging during fusion of single synaptic vesicles with the acceptor SNARE planar membrane is characterized by a sharp increase of the fluorescence intensity followed by an immediate decrease of the peak intensity and a delayed decrease of the mean intensity caused by the diffusion of Rh-DOPE out of the region of interest. The sharp increase is caused by the orientation change of the fluorophor in the evanescent field of the s-polarized laser light (28) and dequenching of rhodamine as it spreads into the supported membrane. Fig. 1, *A–C* show three fusion events that differ in their delay times between docking and fusion. Fig. 1 *D* represents an example of a docking event without subsequent fusion. We quantified the fusion efficiency by the fraction of vesicles that fused with the planar membrane within 1 s after docking. In an average of five experiments, (21 ± 11) % of vesicles fused in the absence of any divalent cations, (43 ± 7) % of vesicles fused in the presence of

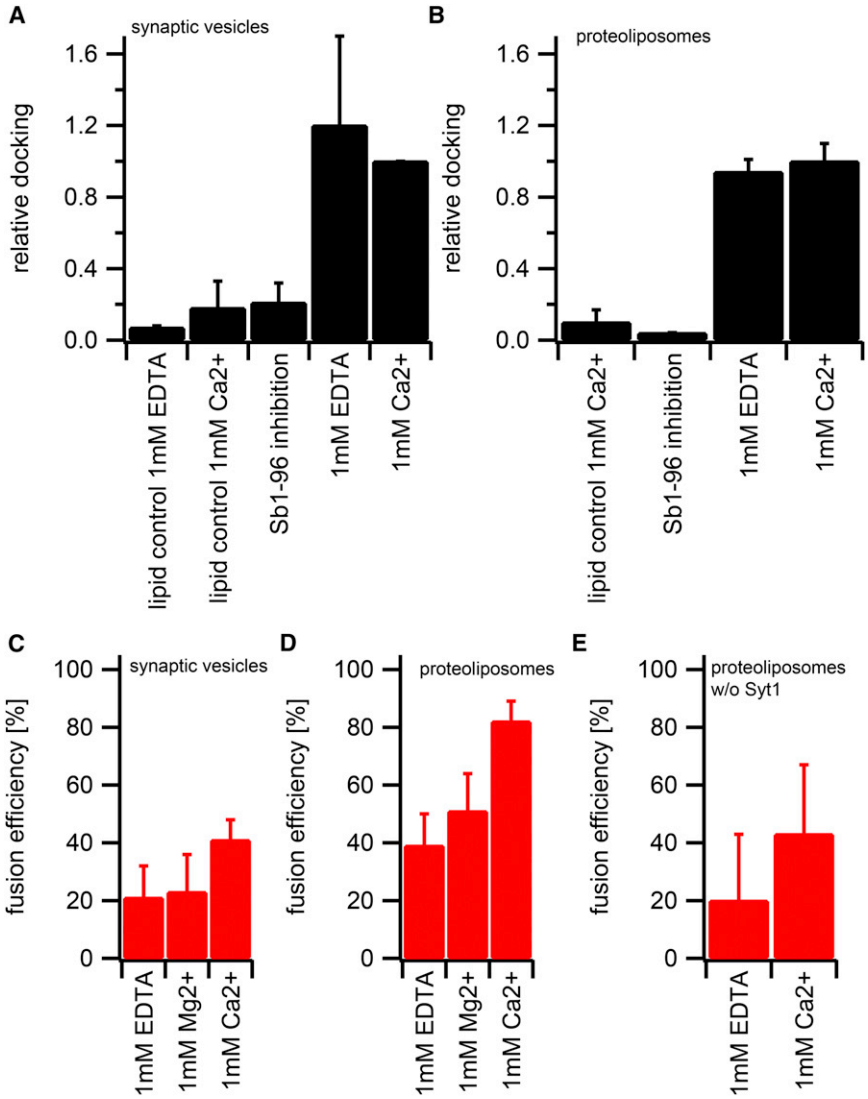

FIGURE 2 Docking of synaptic vesicles and proteoliposomes is SNARE specific. Fusion efficiencies are Ca^{2+}-dependent. (*A*) Docking of synaptic vesicles to supported membranes, in the presence and absence of the acceptor SNARE complex, with and without 1 mM Ca^{2+} and in the presence of the soluble SNARE motif containing fragment Syb1–96 of Syb2. Number of observed docking events during the first 8–10 min of each experiment is normalized to the result in the presence of 1 mM Ca^{2+} and averaged between 4 and 13 experiments. (*B*) Docking of proteoliposomes comprising Syb2 (l/p 300) and Syt1 (l/p 1000) to supported membranes, in the presence and absence of the acceptor SNARE complex, with and without 1 mM Ca^{2+} and in the presence of the soluble SNARE motif containing fragment Syb1–96 of Syb2. Final docking densities were determined from the total fluorescence at the membrane after saturation (Eq. 1), averaged between 6 and 8 experiments and normalized to the result in the presence of 1 mM Ca^{2+}. (*C*) Fraction of synaptic vesicles that fused with acceptor SNARE complex-containing supported membranes within 500 ms after docking in the presence and absence of 1 mM Ca^{2+} or 1 mM Mg^{2+}. (*D*) Fraction of proteoliposomes comprising Syb2 (l/p 300) and Syt1 (l/p 1000) that fused with acceptor SNARE complex-containing supported membranes in the presence and absence of 1 mM Ca^{2+} or 1 mM Mg^{2+}. (*E*) Fraction of proteoliposomes containing Syb2 (l/p 300) only that fused with acceptor SNARE complex-containing supported membranes in the presence and absence of 1 mM Ca^{2+}. Error bars represent standard deviations between different experiments. The *p* values for the statistical differences between docking with and without Ca^{2+} are 0.009 for the synaptic vesicles, 0.001 for the proteoliposomes with Syt1, and 0.1 for the proteoliposomes without Syt1.

1 mM Ca^{2+} and (23 ± 13) % of vesicles fused in the presence of 1 mM Mg^{2+} (Fig. 2 *C*).

The clear distinction between the time of docking and the onset of fusion allowed us to analyze the kinetics of vesicle fusion in our assay. Fig. 3 *A* shows the normalized cumulative distributions from 100 fusion events in the absence of divalent cations and 235 fusion events in the presence of 1 mM Ca^{2+} together with the best fit curves to a first-order kinetics equation. In the presence and absence of Ca^{2+}, the time constants for the onset of fusion after membrane docking were (36 ± 2) ms and (63 ± 6) ms, respectively.

Considering that the effects of Ca^{2+} are moderate, particularly when considering that Ca^{2+} accelerates synaptic exocytosis by more than four orders of magnitude (29), we were interested in determining if the observed Ca^{2+} effects on fusion were specific for Ca^{2+}. Therefore, we carried out control experiments in the presence of Mg^{2+}. We fitted a first-order kinetic curve to the fusion delay time distribution and obtained a time constant of (34 ± 2) ms, almost identical to the previously presented result in the presence of 1 mM Ca^{2+} (Fig. 3 *A*). Thus, we conclude that the acceleration of the fusion kinetic is of electrostatic origin. In additional experiments, we used a simpler acceptor SNARE membrane without any charged lipids consisting only of 1-palmitoyl-2-oleoyl phosphatidylcholine (POPC) and cholesterol (4:1). In these cases, Ca^{2+} had no effect on the fusion kinetics, confirming the electrostatic origin of the observed acceleration in the presence of anionic lipids (see Fig. S2 in the Supporting Material).

Proteoliposome fusion kinetics are more complex and their Ca^{2+}-dependence is more pronounced than synaptic vesicle fusion

To assess how fast synaptic vesicle fusion compares with fast fusion of reconstituted proteoliposomes, we repeated

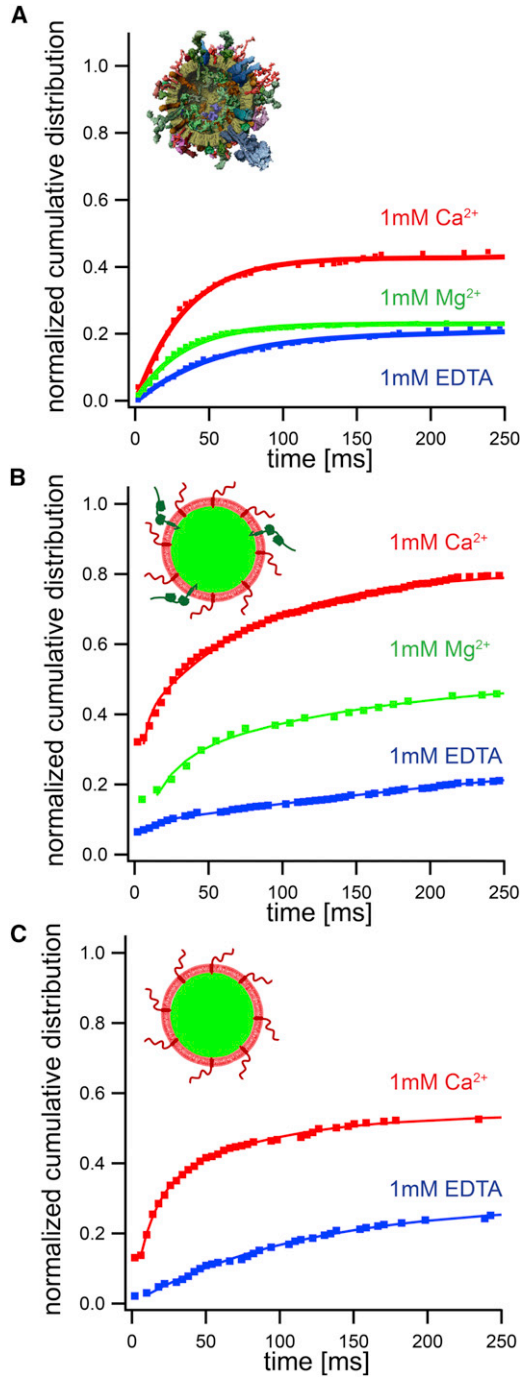

FIGURE 3 Kinetics of membrane fusion of synaptic vesicles and proteoliposomes fusing with acceptor SNARE complex-containing supported membranes in the presence and absence of divalent cations. The cumulative distribution functions (CDF) of time lags between docking and the onset of fusion were constructed and normalized to the fitted saturation value and the fusion efficiency under each condition. (*A*) The CDFs of time lags for synaptic vesicle fusion with acceptor SNARE complex-containing supported membranes from 235 events in the presence of 1 mM Ca^{2+} (*red*), from 275 events in the presence of 1 mM Mg^{2+} (*green*), and from 100 events in the presence of 1 mM EDTA (*blue*). First-order kinetics with time constants of (36 ± 2) ms (1 mM Ca^{2+}), (34 ± 2) ms (1 mM Mg^{2+}), and (63 ± 6) ms (1 mM EDTA) were fitted to the data. (*B*) CDFs of time lags of Syb2 and Syt1-containing proteoliposomes fusing with acceptor SNARE complex-containing supported membranes in the presence of 1 mM Ca^{2+} (*red*) 1 mM Mg^{2+} (*green*), and 1 mM EDTA (*blue*). Two fraction first-order kinetics were fitted to the data. In the presence of 1 mM Ca^{2+} 45% of proteoliposomes fused with a characteristic time constant of (4.1 ± 0.6) ms, whereas 55% fused with a time constant of (77.9 ± 0.8) ms. In the presence of 1 mM Mg^{2+} 48% of proteoliposomes fused with a characteristic time constant of (17 ± 2) ms, whereas 52% fused with a time constant of (200 ± 150) ms. In the presence of 1 mM EDTA, 22% of proteoliposomes fused with a characteristic time constant of (5.1 ± 0.2) ms, whereas 78% fused with a time constant of (450 ± 300) ms. (*C*) CDFs of time lags of Syb2-containing proteoliposomes fusing with acceptor SNARE complex-containing supported membranes in the presence of 1 mM Ca^{2+} (*red*) and 1 mM EDTA (*blue*). Two fractions and single fraction first-order kinetics were fitted to the data. In the presence of 1 mM Ca^{2+}, 56% of proteoliposomes fused with a characteristic time constant of (12 ± 4) ms, whereas 44% fused with a time constant of (80 ± 50) ms. In the presence of 1 mM EDTA, a single fraction first-order kinetics fit revealed a characteristic time constant of (120 ± 15) ms.

the experiments and replaced the synaptic vesicles with liposomes containing the lipids bPC, bPE, bPS, and cholesterol (24:30:5:40) as well as the synaptic vesicle membrane proteins Syb2 (p/l 1:300) and Syt1 (p/l 1:1000). These relative protein and lipid species concentrations are all close to their physiological concentrations in synaptic vesicles (22).

Docking was quantified as previously described (17). Like synaptic vesicles, proteoliposome docking to supported membranes was SNARE specific (Fig. 2 *B*). As with synaptic vesicles, we extracted and analyzed the fluorescence intensity traces from docked proteoliposomes. These traces show the same characteristics as the examples in Fig. 1 and as previously described (28). To confirm that membrane mixing occurs at the same time as fusion pore opening, we performed additional experiments with the encapsulated content dye sulforhodamine. In these cases, the membrane was labeled with the fluorescent lipid analog DiD. These experiments confirmed that pore opening coincides with the sharp increase in membrane dye fluorescence (Fig. S1). Fusion efficiencies were about twice as high as with synaptic vesicles. (39 ± 15) % of docked proteoliposomes fused in the absence and (82 ± 13) % of docked proteoliposomes fused in the presence of Ca^{2+}. When we added 1 mM Mg^{2+} to the proteoliposomes, we observed a slight increase in fusion efficiency to (51 ± 8) % (Fig. 2 *D*). The cumulative distributions from 229 fusion events without Ca^{2+} and 1128 fusion events with Ca^{2+} are shown in Fig. 3 *B*. We were not able to fit a simple first order kinetic to these data. Instead it was necessary to include a second fraction. In the absence of Ca^{2+}, 22% of liposomes fused with a time constant of (5.1 ± 0.2) ms, whereas the remaining 78% fused with a time constant of (450 ± 300) ms, leading to a weighted average fusion time of 352 ms. In the presence of 1 mM Ca^{2+}, the fast fraction increased to 45% and fused with a time constant of (4.1 ± 0.6) ms, whereas the slow fraction decreased to 55% and fused with a time constant of (77.9 ± 0.8) ms. The weighted average fusion time in the presence of Ca^{2+} was 44.7 ms.

Analyzing the fusion kinetics in the presence of Mg^{2+} revealed that 48% of the liposomes fused fast with a time constant of (17 ± 2) ms, i.e., only slightly slower than in the presence of Ca^{2+}. Liposomes in the slow fraction fused with a time constant of (200 ± 150) ms; the weighted average fusion time in the presence of Mg^{2+} was 112 ms.

Synaptobrevin only liposomes show less calcium dependence

The data described above indicate that, in contrast to synaptic vesicles, there appears to be a moderate, albeit significant effect of Ca^{2+} on fusion efficiency, which is not mimicked by Mg^{2+}. To find out whether Syt1 is responsible for this effect, we repeated the experiments using proteoliposomes containing only the synaptic vesicle membrane protein Syb2, but under otherwise identical conditions. Fusion efficiencies of proteoliposomes with only Syb2 were about half of those that also contained Syt1. Although the range of fusion efficiencies between experiments was larger than before, the average fusion efficiency in the presence of 1 mM Ca^{2+} was still higher than in the absence of Ca^{2+} (Fig. 2 *E*). Analyzing the fusion kinetics revealed that fusion occurred with a typical time constant of (120 ± 15) ms in the absence of Ca^{2+}. In the presence of Ca^{2+}, 56% of events fused with a time constant of (12 ± 4) ms, whereas the remaining 44% fused with a time constant of (80 ± 50) ms (Fig. 3 *C*), leading to a weighted average fusion time of 42 ms. Although not as pronounced, about half of the proteoliposome fusion events remain Ca^{2+}-dependent even without Syt1.

DISCUSSION

Reconstitution of the essential neuronal SNAREs in a functional assay lead to the crucial validation of the SNARE hypothesis (1) and evolving more sophisticated fusion assays with reconstituted components account for much of the more recent progress in the field (8,9,12,30). Recently, we found that even relatively simple changes to the lipid composition of synaptic vesicle-mimicking proteoliposomes that interact with supported membranes influence docking and fusion efficiencies as well as the kinetics of the fusion reaction (26). To demonstrate that appropriately reconstituted proteoliposomes mimic the fusion activity of synaptic vesicles, we replaced in this work the reconstituted proteoliposomes entirely with natural, intact synaptic vesicles that were purified from rat brain. The most important conclusion from this study is that native synaptic vesicles with their complex membranes behave in many ways very similar to their reconstituted counterparts with regard to docking and fusion to model membranes. The corollary of this conclusion is that fusion previously observed with reconstituted vesicles with millisecond time resolution faithfully reproduces fusion of native synaptic vesicles.

Docking, defined here as the SNARE-specific immobilization of vesicles at the supported membrane surface, depends on the presence of an appropriately reconstituted and likely a laterally diffusing acceptor SNARE complex in the supported target membrane. Omitting critical components or adding the soluble SNARE domain of synaptobrevin (Syb1–96) to the acceptor SNARE complex abolishes binding of both synaptic vesicles and proteoliposomes. Once docked, fluorescence dissipated from fusing vesicles with the same signature patterns for synaptic as well as reconstituted vesicles (17,28), suggesting that reconstituted and native vesicles fuse with planar membranes using a similar mechanism.

Up to 48% of the docked synaptic vesicles fused within 250 ms after docking. Again, this fusion efficiency is similar to the fusion efficiency of proteoliposomes in this and our previously published work (17,26). Most of these synaptic vesicles and proteoliposomes fuse within 20 to 50 ms to acceptor SNARE-containing supported membranes. However, although the distribution of synaptic vesicle fusion times is very homogenous such that they could be fitted with a single fraction first order kinetic rate law, the proteoliposomes showed two distinct fractions. A possible explanation for this special feature, which is only observed with the proteoliposomes, is that fusion-competent Syb2 might be in conformational exchange with a fusion-incompetent fraction on the surface of proteoliposomes, but better regulated for fusion-release by synaptophysin on synaptic vesicles (31,32). Although similar amounts of cholesterol were included in the reconstituted vesicles as present in synaptic vesicles, the lateral distribution of fusion competent Syb2 may also be different in the two systems.

The two kinetic components cannot be a result of the use of an acceptor t-SNARE complex that contains the C-terminal SNARE motif peptide of synaptobrevin (27). This peptide was included to prevent the detrimental formation of a 2:1 Syx/SNAP-25 complex, which inevitably is formed in standard reconstitution procedures and which prevents efficient fast fusion because one Syx1a must first be released before Syb2 can form an active SNARE complex. Nevertheless, it is important to note that the fastest kinetics that we observe with synaptic vesicles or proteoliposomes is likely still limited by the displacement of the C-terminal Syb49–96 peptide in the acceptor SNARE complex after the ternary SNARE complex is nucleated at the N-terminal end of the SNARE motif (30,33). Therefore, all fusion times reported in this work, even if they are among the fastest of any SNARE reconstitution so far reported in the literature, must still be considered upper limits. It is likely that the actual fusion reaction, i.e., the membrane merger after release of the short peptide, proceeds at still higher rates in our system, perhaps even as fast as in a few hundred microseconds, i.e., the known speed of neurotransmitter release at synapses (34,35). Although a single SNARE complex can be sufficient to catalyze fusion in highly curved

model membranes (36), more SNARE complexes are likely required to support fast fusion with a planar target membrane (17,26,30,37). Consistent with this idea, Mohrmann et al (38) found that a single SNARE complex might be sufficient to promote sustained slow fusion in chromaffin cells, whereas three or more were needed to support fast fusion reactions in these cells.

Because the purified synaptic vesicles contain the membrane protein Syt1, which is the calcium sensor that initiates fast evoked neurotransmitter release at the synapse, we compared results from experiments with and without Ca^{2+} and performed proteoliposome experiments with and without reconstituted recombinant Syt1. The biological and reconstituted membranes both showed increased fusion efficiencies and accelerated fusion in the presence of divalent cations. These accelerated kinetics depended on the presence of anionic lipids in the supported membrane, which means that the observed acceleration of synaptic and reconstituted vesicle fusion is at least partially electrostatic and anionic lipid mediated. This is confirmed with experiments using Mg^{2+}, which mimics the electrostatic component of Ca^{2+}, but does not specifically bind to the Ca^{2+}-binding loops of Syt1. Because Mg^{2+} reproduced part, but not all of the Ca^{2+}-mediated enhancement in the fusion efficiency, we conclude that there are electrostatic and Ca^{2+}-Syt1 specific components that enhance the SNARE-mediated fusion efficiency. Consistent with this dual role of Ca^{2+}, proteoliposomes that contained Syt1 in addition to Syb2 showed an additional acceleration and further increased fusion efficiency in the presence of Ca^{2+}. Reasons for the complex fusion behavior observed with proteoliposomes in the presence of Syt1 may be due to the back-binding of the Syt1 C2 domains to their own membrane (10,39,40). In addition, the PIP_2 distribution in the target membrane may be quite critical to observe a strong synaptotagmin-mediated Ca^{2+} effect on fusion, which may explain contradicting reports in the literature regarding this effect (8,9,41).

It is important to reiterate that the fusion kinetics that we determine in our assay describe the reaction times between capturing the vesicles on the membrane and the onset of fusion. The docked state in this assay and, indeed, in all reconstituted liposome fusion assays, is purely SNARE mediated and thus does not necessarily represent the physiological docked and primed state. Primed vesicles in the synapse are ready to fuse, catalyzed by synaptotagmin and Ca^{2+}. It is still not clear if engagement of synaptotagmin with proteins and lipids of the fusion machinery occurs upstream (11), downstream (42), or at both points relative to the first SNARE interactions. Although the presented hybrid system consisting of a (complex) native synaptic vesicle membrane and a (simplified) supported membrane does not reproduce the high temporal and spatial organization of the fusion site yet, it constitutes a significant step forward in closing the gap between biochemistry and physiology. Parts that are still missing in our quest to reproduce and understand physiological fusion must include components that block the synaptic vesicles (or proteoliposomes) from proceeding through full fusion before the Ca^{2+} signal arrives. An important goal of future research must be to discover these missing parts to fully understand how Ca^{2+} unleashes neurotransmitter release on the submillisecond timescale.

CONCLUSION

The results of this report clearly show that synaptic vesicles can undergo rapid fusion with appropriately reconstituted acceptor SNARE target membranes and that reconstituted proteoliposomes can substitute to a large degree as appropriate mimics of native synaptic vesicles in fast single-vesicle fusion assays. The synaptic vesicles in this hybrid in vitro assay are closer to the physiological situation in cells and may have advantages in further dissecting requirements on the target membrane for optimal fusion. However, using reconstituted proteoliposomes in the single vesicle-to-planar-membrane fusion assays has the advantage of their relatively easy preparation and labeling procedures while permitting the simultaneous monitoring of lipid and content mixing. We are optimistic that by further fine-tuning this system, particularly on the supported membrane side, future work will elucidate the true inner workings of the synaptic fusion machine.

SUPPORTING MATERIAL

Two figures and their legends are available at http://www.biophysj.org/biophysj/supplemental/S0006-3495(13)00377-9.

This work was supported by grant P01 GM72694 from the National Institutes of Health.

REFERENCES

1. Weber, T., B. V. Zemelman, …, J. E. Rothman. 1998. SNAREpins: minimal machinery for membrane fusion. *Cell.* 92:759–772.

2. Schuette, C. G., K. Hatsuzawa, …, R. Jahn. 2004. Determinants of liposome fusion mediated by synaptic SNARE proteins. *Proc. Natl. Acad. Sci. USA.* 101:2858–2863.

3. Tucker, W. C., T. Weber, and E. R. Chapman. 2004. Reconstitution of Ca2+-regulated membrane fusion by synaptotagmin and SNAREs. *Science.* 304:435–438.

4. Xu, Y., F. Zhang, …, Y. K. Shin. 2005. Hemifusion in SNARE-mediated membrane fusion. *Nat. Struct. Mol. Biol.* 12:417–422.

5. Chen, X., D. Araç, …, J. Rizo. 2006. SNARE-mediated lipid mixing depends on the physical state of the vesicles. *Biophys. J.* 90:2062–2074.

6. Dennison, S. M., M. E. Bowen, …, B. R. Lentz. 2006. Neuronal SNAREs do not trigger fusion between synthetic membranes but do promote PEG-mediated membrane fusion. *Biophys. J.* 90:1661–1675.

7. Bhalla, A., M. C. Chicka, …, E. R. Chapman. 2006. Ca2+-synaptotagmin directly regulates t-SNARE function during reconstituted membrane fusion. *Nat. Struct. Mol. Biol.* 13:323–330.
8. Lee, H. K., Y. Yang, …, T. Y. Yoon. 2010. Dynamic Ca2+-dependent stimulation of vesicle fusion by membrane-anchored synaptotagmin 1. *Science.* 328:760–763.
9. Kyoung, M., A. Srivastava, …, A. T. Brunger. 2011. In vitro system capable of differentiating fast Ca2+-triggered content mixing from lipid exchange for mechanistic studies of neurotransmitter release. *Proc. Natl. Acad. Sci. USA.* 108:E304–E313.
10. Stein, A., A. Radhakrishnan, …, R. Jahn. 2007. Synaptotagmin activates membrane fusion through a Ca2+-dependent *trans* interaction with phospholipids. *Nat. Struct. Mol. Biol.* 14:904–911.
11. van den Bogaart, G., S. Thutupalli, …, R. Jahn. 2011. Synaptotagmin-1 may be a distance regulator acting upstream of SNARE nucleation. *Nat. Struct. Mol. Biol.* 18:805–812.
12. Malsam, J., D. Parisotto, …, T. H. Söllner. 2012. Complexin arrests a pool of docked vesicles for fast Ca2+-dependent release. *EMBO J.* 31:3270–3281.
13. Diao, J., P. Grob, …, A. T. Brunger. 2012. Synaptic proteins promote calcium-triggered fast transition from point contact to full fusion. *eLife.* 1:e00109.
14. Bowen, M. E., K. Weninger, …, S. Chu. 2004. Single molecule observation of liposome-bilayer fusion thermally induced by soluble N-ethyl maleimide sensitive-factor attachment protein receptors (SNAREs). *Biophys. J.* 87:3569–3584.
15. Liu, T., W. C. Tucker, …, J. C. Weisshaar. 2005. SNARE-driven, 25-millisecond vesicle fusion in vitro. *Biophys. J.* 89:2458–2472.
16. Yoon, T. Y., B. Okumus, …, T. Ha. 2006. Multiple intermediates in SNARE-induced membrane fusion. *Proc. Natl. Acad. Sci. USA.* 103:19731–19736.
17. Domanska, M. K., V. Kiessling, …, L. K. Tamm. 2009. Single vesicle millisecond fusion kinetics reveals number of SNARE complexes optimal for fast SNARE-mediated membrane fusion. *J. Biol. Chem.* 284:32158–32166.
18. Karatekin, E., J. Di Giovanni, …, J. E. Rothman. 2010. A fast, single-vesicle fusion assay mimics physiological SNARE requirements. *Proc. Natl. Acad. Sci. USA.* 107:3517–3521.
19. Verhage, M., and J. B. Sørensen. 2008. Vesicle docking in regulated exocytosis. *Traffic.* 9:1414–1424.
20. Fasshauer, D., W. Antonin, …, R. Jahn. 1999. Mixed and non-cognate SNARE complexes. Characterization of assembly and biophysical properties. *J. Biol. Chem.* 274:15440–15446.
21. Fasshauer, D., and M. Margittai. 2004. A transient N-terminal interaction of SNAP-25 and syntaxin nucleates SNARE assembly. *J. Biol. Chem.* 279:7613–7621.
22. Takamori, S., M. Holt, …, R. Jahn. 2006. Molecular anatomy of a trafficking organelle. *Cell.* 127:831–846.
23. Kalb, E., S. Frey, and L. K. Tamm. 1992. Formation of supported planar bilayers by fusion of vesicles to supported phospholipid monolayers. *Biochim. Biophys. Acta.* 1103:307–316.
24. Wagner, M. L., and L. K. Tamm. 2000. Tethered polymer-supported planar lipid bilayers for reconstitution of integral membrane proteins: silane-polyethyleneglycol-lipid as a cushion and covalent linker. *Biophys. J.* 79:1400–1414.
25. Kiessling, V., J. M. Crane, and L. K. Tamm. 2006. Transbilayer effects of raft-like lipid domains in asymmetric planar bilayers measured by single molecule tracking. *Biophys. J.* 91:3313–3326.
26. Domanska, M. K., V. Kiessling, and L. K. Tamm. 2010. Docking and fast fusion of synaptobrevin vesicles depends on the lipid compositions of the vesicle and the acceptor SNARE complex-containing target membrane. *Biophys. J.* 99:2936–2946.
27. Pobbati, A. V., A. Stein, and D. Fasshauer. 2006. N- to C-terminal SNARE complex assembly promotes rapid membrane fusion. *Science.* 313:673–676.
28. Kiessling, V., M. K. Domanska, and L. K. Tamm. 2010. Single SNARE-mediated vesicle fusion observed in vitro by polarized TIRFM. *Biophys. J.* 99:4047–4055.
29. Neher, E., and T. Sakaba. 2008. Multiple roles of calcium ions in the regulation of neurotransmitter release. *Neuron.* 59:861–872.
30. Hernandez, J. M., A. Stein, …, R. Jahn. 2012. Membrane fusion intermediates via directional and full assembly of the SNARE complex. *Science.* 336:1581–1584.
31. Reisinger, C., S. V. Yelamanchili, …, G. Ahnert-Hilger. 2004. The synaptophysin/synaptobrevin complex dissociates independently of neuroexocytosis. *J. Neurochem.* 90:1–8.
32. Willig, K. I., S. O. Rizzoli, …, S. W. Hell. 2006. STED microscopy reveals that synaptotagmin remains clustered after synaptic vesicle exocytosis. *Nature.* 440:935–939.
33. Gao, Y., S. Zorman, …, Y. Zhang. 2012. Single reconstituted neuronal SNARE complexes zipper in three distinct stages. *Science.* 337:1340–1343.
34. Schneggenburger, R., and E. Neher. 2000. Intracellular calcium dependence of transmitter release rates at a fast central synapse. *Nature.* 406:889–893.
35. Wolfel, M., and R. Schneggenburger. 2003. Presynaptic capacitance measurements and Ca2+ uncaging reveal submillisecond exocytosis kinetics and characterize the Ca2+ sensitivity of vesicle pool depletion at a fast CNS synapse. *J. Neurosci.* 23:7059–7068.
36. van den Bogaart, G., M. G. Holt, …, R. Jahn. 2010. One SNARE complex is sufficient for membrane fusion. *Nat. Struct. Mol. Biol.* 17:358–364.
37. Shi, L., Q. T. Shen, …, F. Pincet. 2012. SNARE proteins: one to fuse and three to keep the nascent fusion pore open. *Science.* 335:1355–1359.
38. Mohrmann, R., H. de Wit, …, J. B. Sørensen. 2010. Fast vesicle fusion in living cells requires at least three SNARE complexes. *Science.* 330:502–505.
39. Vennekate, W., S. Schröder, …, P. J. Walla. 2012. *Cis*- and *trans*-membrane interactions of synaptotagmin-1. *Proc. Natl. Acad. Sci. USA.* 109:11037–11042.
40. Park, Y., J. M. Hernandez, …, R. Jahn. 2012. Controlling synaptotagmin activity by electrostatic screening. *Nat. Struct. Mol. Biol.* 19:991–997.
41. Kim, J. Y., B. K. Choi, …, N. K. Lee. 2012. Solution single-vesicle assay reveals PIP2-mediated sequential actions of synaptotagmin-1 on SNAREs. *EMBO J.* 31:2144–2155.
42. Giraudo, C. G., W. S. Eng, …, J. E. Rothman. 2006. A clamping mechanism involved in SNARE-dependent exocytosis. *Science.* 313: 676–680.